

**Nonadiabatic dynamics simulations of singlet fission in
2,5-bis(fluorene-9-ylidene)-2,5-dihydrothiophene
crystals.**

Supporting Information.

Meilani Wibowo^{a,b}, Maurizio Persico^{a,*}, Giovanni Granucci^a

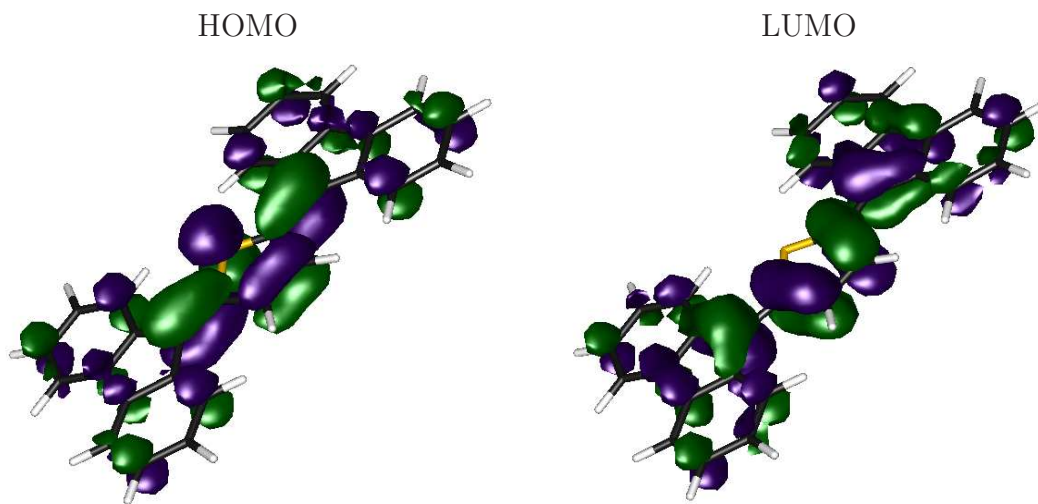
^a Dipartimento di Chimica e Chimica Industriale, Università di Pisa,
v. G. Moruzzi, I-56124 Pisa, Italy

^b Theoretical Chemistry, Zernike Institute for Advanced Materials, University
of Groningen, Nijenborgh 4, 9747 AG Groningen, The Netherlands

Molecular orbitals and transition dipole moment.

Fig. S1 shows the HOMO and LUMO orbitals of ThBF, as computed at FOMO-CI level. At the equilibrium geometry the point group is C_s , with a symmetry plane that divides the molecule in half and contains the sulphur atom. The HOMO is a' and the LUMO is a'' , so the $S_0 \rightarrow S_1$ transition dipole is perpendicular to the symmetry plane. By forcing the molecule in a planar C_{2v} conformation, which is approximately the situation in the crystal, the transition dipole lies in the molecular plane.

Figure S1: HOMO and LUMO orbitals of ThBF.



QM/MM thermal equilibration.

Figs. S2 and S3 allow to monitor different aspects of the progress of the thermal equilibration of the QM/MM cluster.

Figure S2: Total energy (a.u.) as a function of time for the QM/MM cluster.

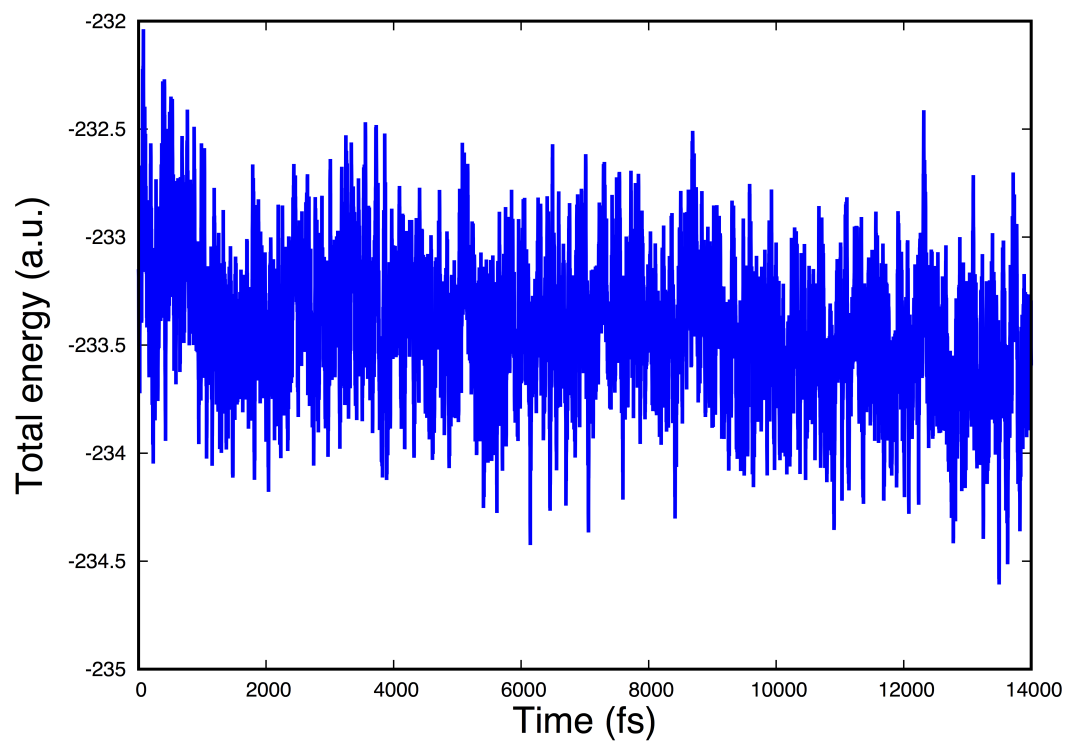
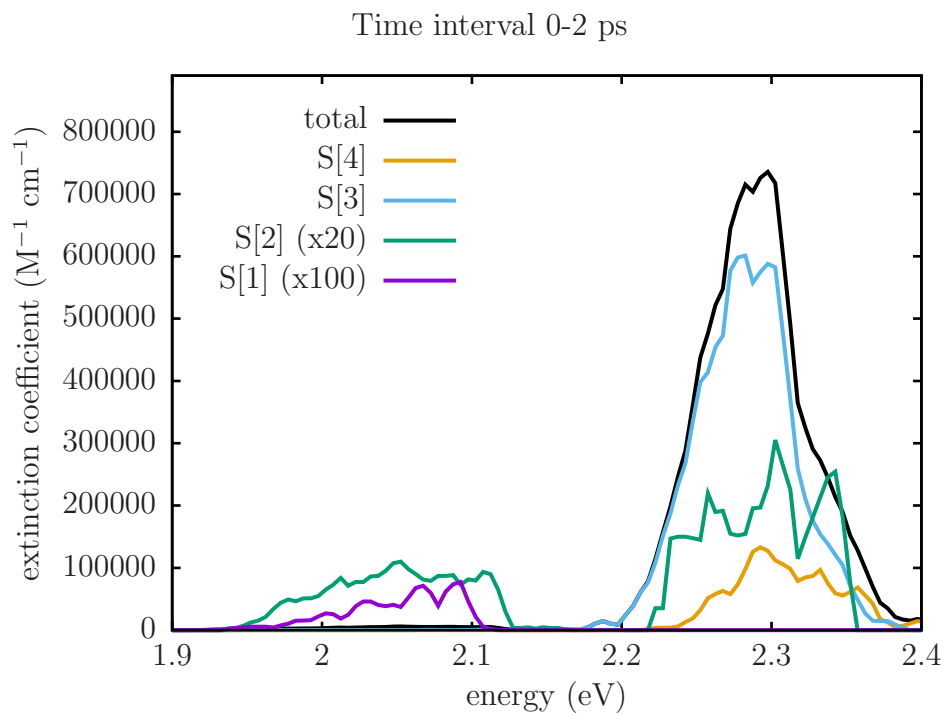
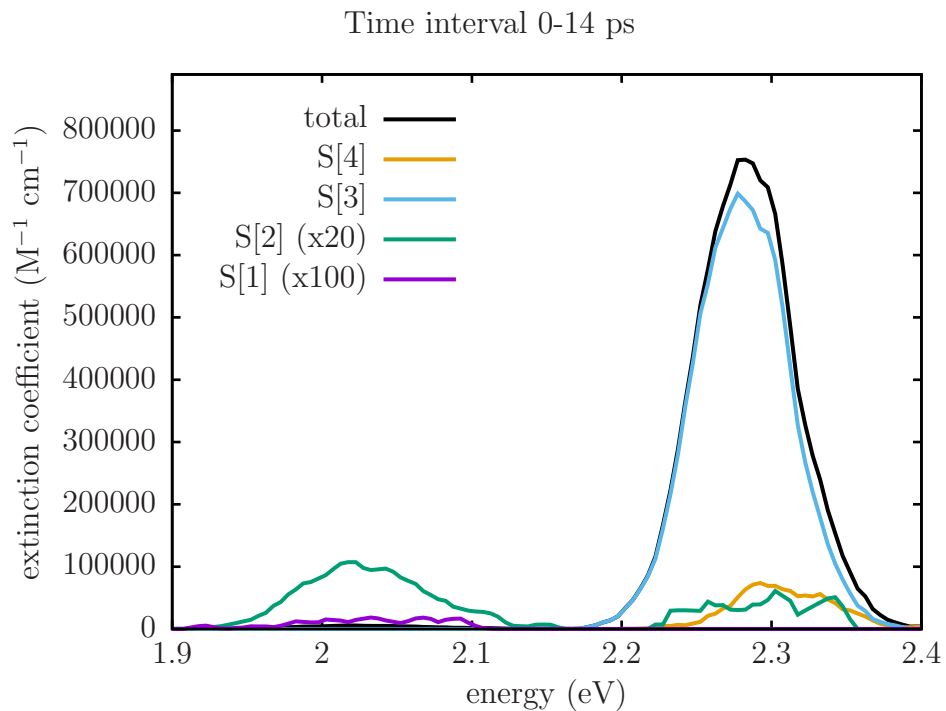
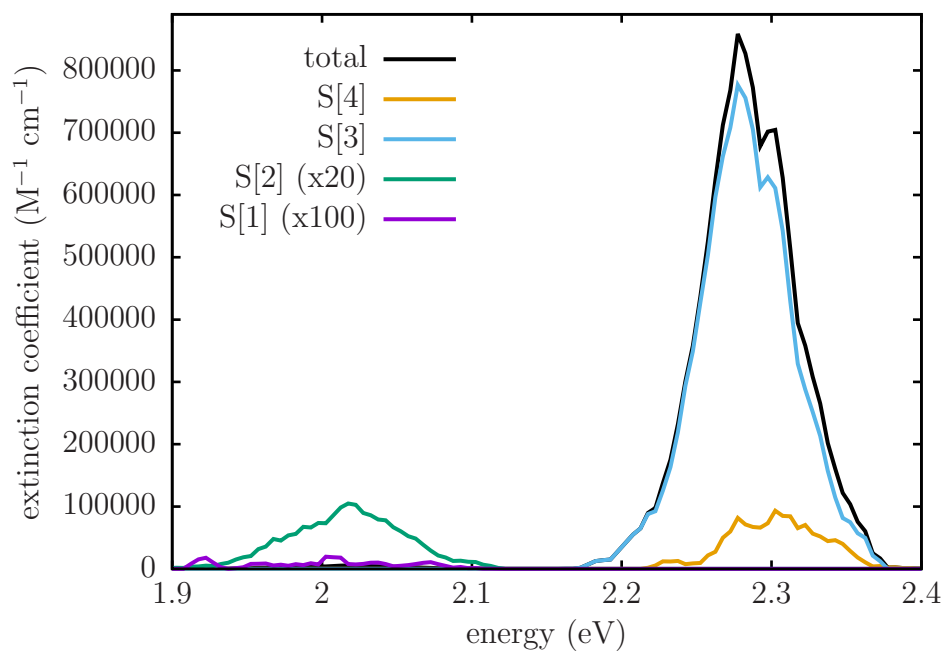


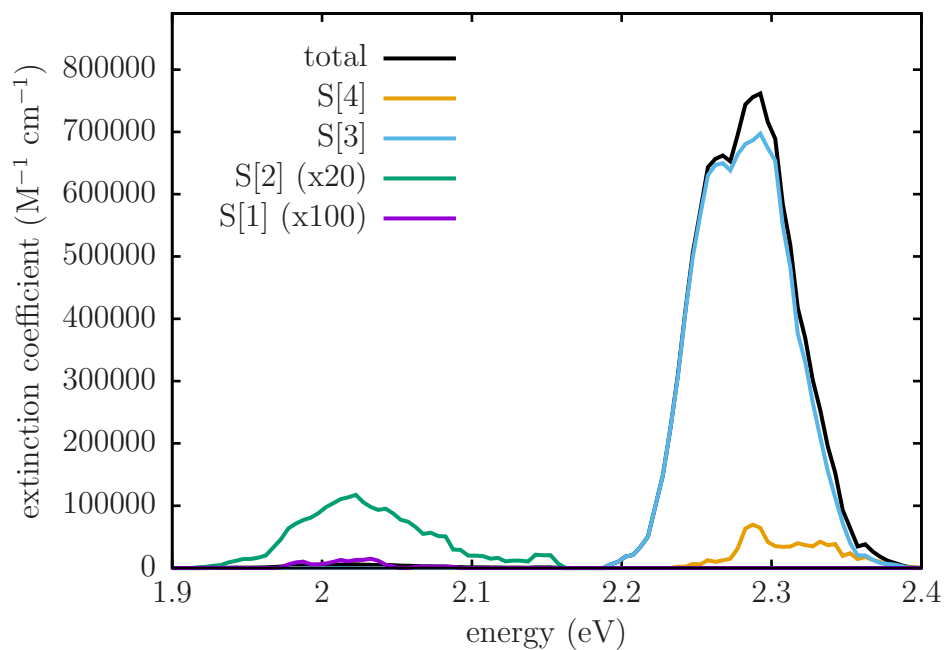
Figure S3: Absorption spectra as obtained by averaging over different time intervals during the thermal equilibration of the QM/MM cluster.



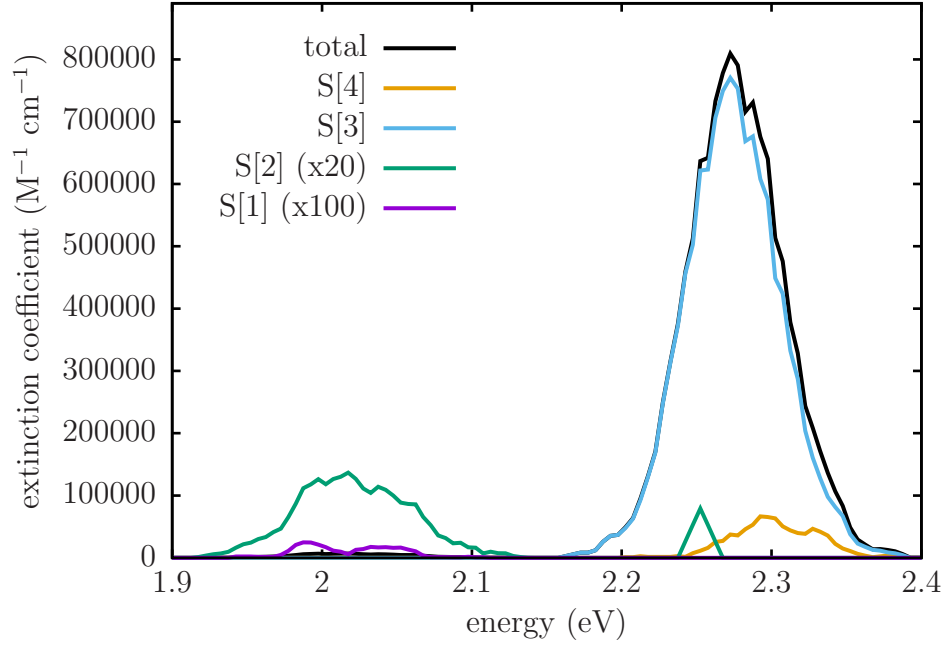
Time interval 2-5 ps



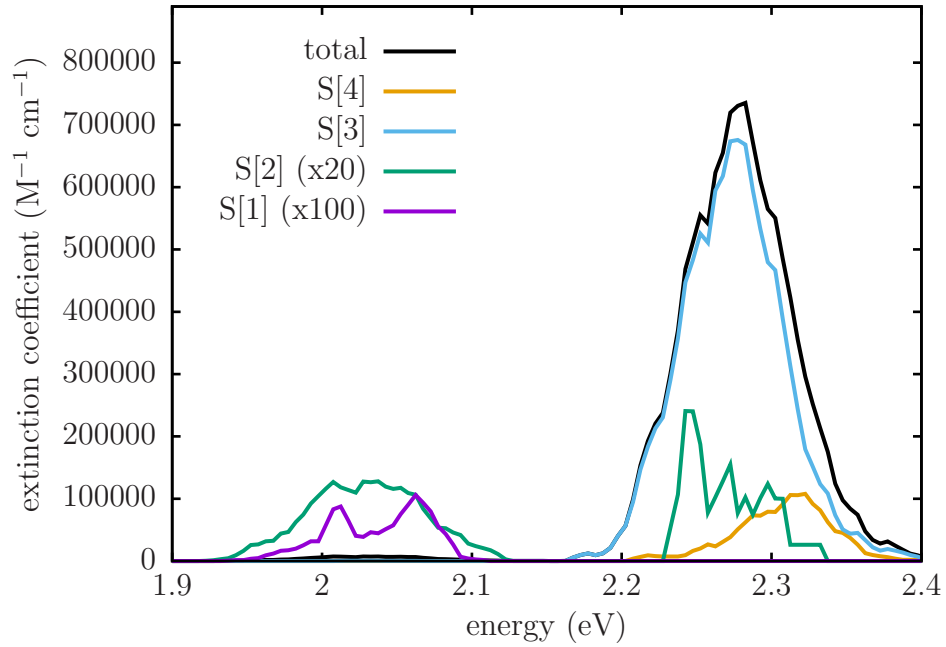
Time interval 5-8 ps



Time interval 8-11 ps



Time interval 11-14 ps



Excited state dynamics. Fig. S4 shows the time dependence of the adiabatic state populations with an expanded time scale, for the first 500 fs. Fig. S5 compares the population of the S[1] state with that of the ^1TT state, computed as the fraction of trajectories where the current state can be identified as ^1TT .

Table S1 is a more detailed version of table 3 in the main text, reporting the transition rates between all pairs of states instead of grouping together the states from S[4] to S[8].

Figure S4: The adiabatic state populations in the first 500 fs.

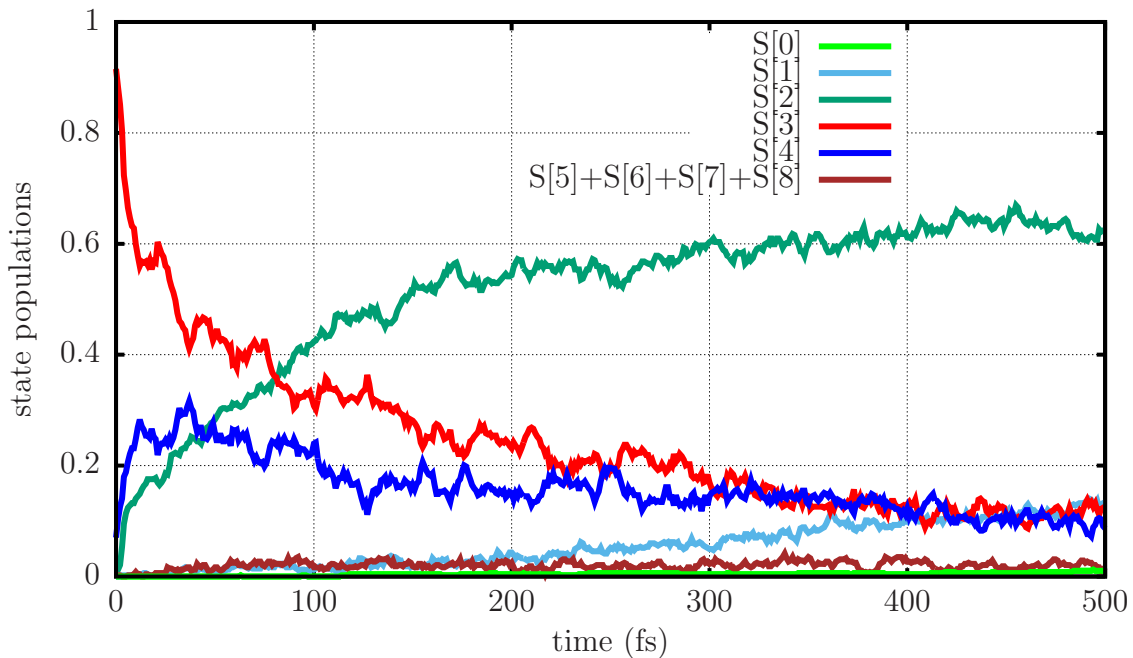


Figure S5: Population of the ${}^1\text{TT}$ state compared with that of the adiabatic state $\text{S}[1]$.

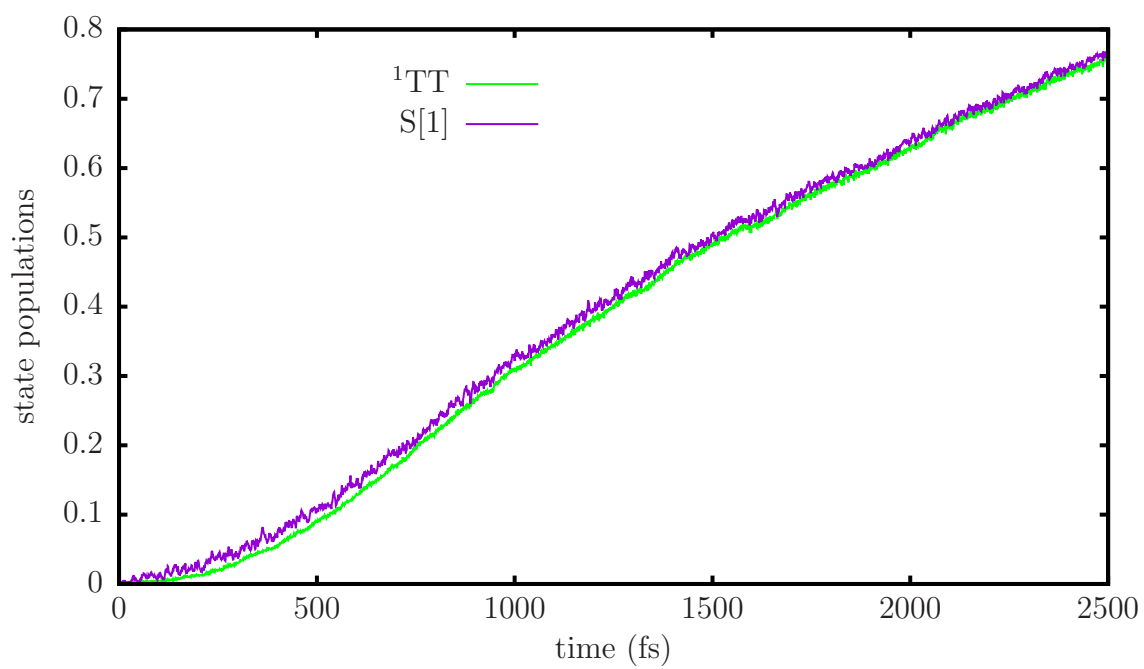


Table S1: Hopping rates (ps^{-1}).

state	state	rate ^a	rate ^a	net
<i>m</i>	<i>n</i>	<i>m</i> → <i>n</i>	<i>n</i> → <i>m</i>	rate ^b
S[1]	S[0]	0.000	0.001	-0.001
S[2]	S[0]	0.042	0.018	0.024
S[3]	S[0]	0.007	0.007	0.000
S[4]	S[0]	0.002	0.009	-0.007
S[5]	S[0]	0.000	0.002	-0.002
S[6]	S[0]	0.005	0.002	0.002
S[7]	S[0]	0.002	0.002	0.000
S[8]	S[0]	0.001	0.002	-0.001
S[2]	S[1]	3.540	3.192	0.349
S[3]	S[1]	0.016	0.031	-0.015
S[4]	S[1]	0.002	0.012	-0.011
S[5]	S[1]	0.001	0.009	-0.008
S[6]	S[1]	0.000	0.006	-0.006
S[7]	S[1]	0.000	0.002	-0.002
S[8]	S[1]	0.000	0.002	-0.002
S[3]	S[2]	3.326	2.165	1.160
S[4]	S[2]	0.796	1.208	-0.412
S[5]	S[2]	0.105	0.340	-0.236
S[6]	S[2]	0.074	0.123	-0.050
S[7]	S[2]	0.042	0.055	-0.013
S[8]	S[2]	0.013	0.031	-0.018
S[4]	S[3]	5.127	4.357	0.770
S[5]	S[3]	0.086	0.062	0.024
S[6]	S[3]	0.050	0.048	0.002
S[7]	S[3]	0.026	0.039	-0.013
S[8]	S[3]	0.014	0.014	0.000
S[5]	S[4]	1.545	1.242	0.302
S[6]	S[4]	0.083	0.047	0.036
S[7]	S[4]	0.025	0.033	-0.008
S[8]	S[4]	0.011	0.018	-0.007
S[6]	S[5]	0.135	0.067	0.068
S[7]	S[5]	0.019	0.007	0.012
S[8]	S[5]	0.002	0.002	-0.001
S[7]	S[6]	0.119	0.070	0.049
S[8]	S[6]	0.012	0.007	0.004
S[8]	S[7]	0.068	0.043	0.025

^a Average rate over the whole simulation in $\text{ps}^{-1} = \frac{\# \text{ hops}}{\# \text{ trajectories} \cdot \text{time}}$

^b Net rate = difference between the $m \rightarrow n$ and the $n \rightarrow m$ rates.

Table S2: Electronic hamiltonian matrix in the basis of 6 low-lying diabatic states for a ThBF dimer, computed with the semiempirical FOMO-CI method. The dimer is made of two ThBF planar molecules at the ground state optimal geometry, with a distance between the two molecular planes of 3.6 Å and a slip of 3.5 Å. Matrix elements in meV.

	$S_0(A)S_0(B)$	1TT	$S_1(A)S_0(B)$	$S_0(A)S_1(B)$	A^-B^+	A^+B^-
$S_0(A)S_0(B)$	0.00	0.22	30.46	-30.46	39.88	-39.88
1TT	0.22	1780.29	0.02	-0.02	-29.41	29.41
$S_1(A)S_0(B)$	30.46	0.02	2148.98	155.06	-18.17	-2.40
$S_0(A)S_1(B)$	-30.46	-0.02	155.06	2148.98	-2.04	-18.17
A^-B^+	39.88	-29.41	-18.17	-2.04	2424.00	0.01
A^+B^-	-39.88	29.41	-2.04	-18.17	0.01	2424.00

Table S3: Comparison of state energies and geometrical parameters at the starting time ($t = 0$) and at the S[2]→S[1] hopping events, averaged over all trajectories.

energy ^a or coordinate ^b	at $t = 0$ (X_0)	at S[2]→S[1] hops (X_h)	difference $X_h - X_0$
ΔE S[1]-S[0]	1.5828	1.3064	-0.2764
ΔE S[2]-S[0]	1.9589	1.3335	-0.6254
ΔE S[2]-S[1]	0.3761	0.0271	-0.3490
ΔE S[3]-S[0]	2.2417	1.8691	-0.3726
ΔE S[3]-S[2]	0.2828	0.5355	0.2527
$\angle C_{13}C_{12}C_{14}C_{15}$	8.8430	9.5528	0.7098
C ₁₂ -C ₁₄	1.3818	1.3841	0.0023
C ₁₄ -C ₁₅	1.4862	1.4838	-0.0025
C ₁₅ -C ₁₆	1.3667	1.3723	0.0056
S	5.6920	5.5042	-0.1879
C ₁₄	5.5513	5.3294	-0.2219
C ₁₅	5.4607	5.2585	-0.2022
C ₁₆	5.4447	5.3397	-0.1050
C ₁₇	5.5534	5.4806	-0.0728
C ₁₂	5.5116	5.2020	-0.3096
C ₇	5.4823	5.3020	-0.1804
C ₄	5.4898	5.3766	-0.1131
C ₉	5.4867	5.1739	-0.3128
C ₂	5.4555	5.2956	-0.1598
C ₁₈	5.5319	5.4807	-0.0512
C ₂₃	5.5988	5.5113	-0.0875
C ₂₆	5.4364	5.4487	0.0124
C ₂₁	5.6505	5.5678	-0.0826
C ₂₈	5.3366	5.3813	0.0447

^a Energy differences in eV between the specified electronic states.

^b Dihedral angle in degrees and distances in Å. For bond lengths within one monomer, two atoms are specified. For distances between an atom of monomer A and the corresponding atom of monomer B, only the former is specified. For atom labelling, refer to Fig. 1.

Simulations taking into account the spin-orbit coupling. The simulation of the excited state dynamics taking into account the spin-orbit coupling (the ‘‘SOC simulation’’) was run by using a more limited sampling of initial conditions, resulting in 66 trajectories, with respect to the singlet-only one described in the main test, which featured a swarm of 484 trajectories. Moreover, it included five singlet states (S[0] to S[4]), whereas the singlet-only simulation had nine (up to S[8]). Figs. 6 and 7 in the main text report the state populations obtained in the singlet-only and SOC simulations, respectively.

Figs. S6 and S7 allow to compare those results with those of two singlet-only simulations using a sampling similar to that of the SOC one: one with five singlet states (Fig. S6) and the other with nine (Fig. S7)

Figure S6: State populations obtained in a singlet-only simulation with five singlet states and a sampling similar to that of the SOC simulation.

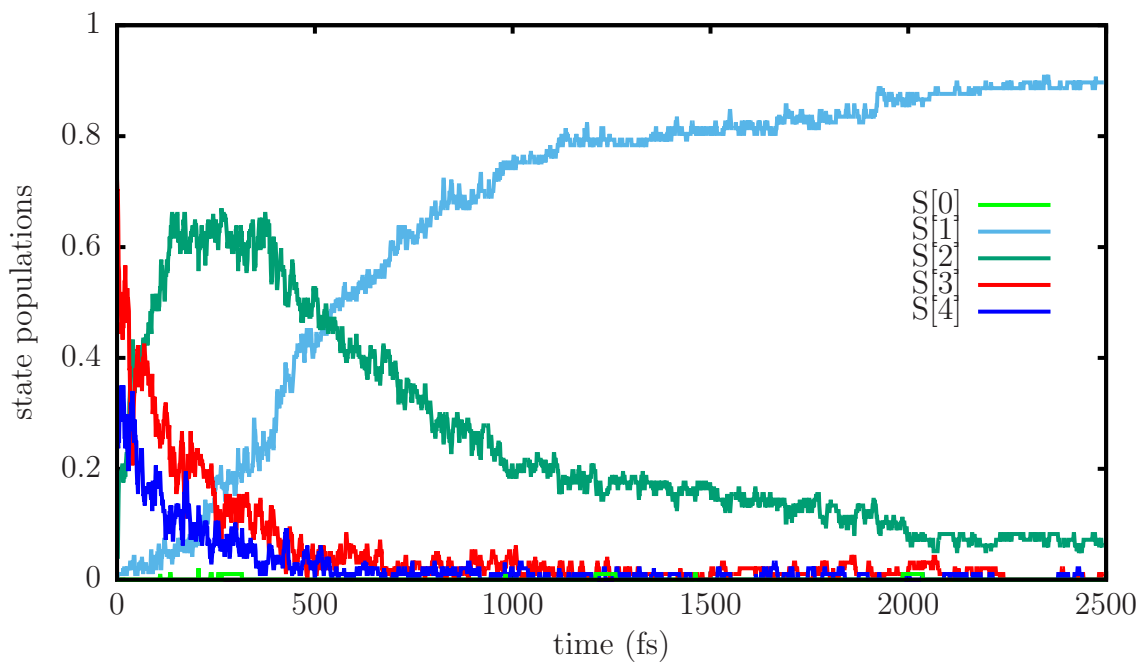


Figure S7: State populations obtained in a singlet-only simulation with nine singlet states and a sampling similar to that of the SOC simulation.

